

Y3, N21/5:6/3872

GOVT. DOC.

BUSINESS AND
TECHNICAL DEPT.

DEC 19 1956

NACA TN 3872

NATIONAL ADVISORY COMMITTEE FOR AERONAUTICS

TECHNICAL NOTE 3872

EXPERIMENTAL DETERMINATION OF THE RANGE OF
APPLICABILITY OF THE TRANSONIC AREA RULE
FOR WINGS OF TRIANGULAR PLAN FORM

By William A. Page

Ames Aeronautical Laboratory
Moffett Field, Calif.



Washington
December 1956



EXPERIMENTAL DETERMINATION OF THE RANGE OF
APPLICABILITY OF THE TRANSONIC AREA RULE
FOR WINGS OF TRIANGULAR PLAN FORM

By William A. Page

SUMMARY

Experimental measurements have been made of the zero-lift drag rise at transonic speeds of a family of triangular plan form wings of varying thickness and aspect ratio mounted on a cylindrical body. Together with the transonic similarity parameters, the results of the tests are used to define the range of applicability of the transonic area rule for wings of triangular plan form. The significance of the test results is discussed.

INTRODUCTION

Since the discovery of the transonic area rule by Whitcomb, a great deal of effort has been expended by many investigators to determine the usefulness and limitations of the rule when applied to a wide variety of aerodynamic shapes. A major point of interest is the degree of slenderness required for the successful application of the area rule. This point has been considered in reference 1 wherein it was shown how the sonic drag-rise values for affinely related wings can be analyzed in terms of the transonic similarity parameters to indicate the range of applicability of the transonic area rule. The method of analysis was applied to available experimental data for a large family of rectangular plan form wings, and the range of geometric variables was found sufficient to define the limitation of the area rule to such wings.

It is the purpose of the present report to extend the knowledge regarding the range of applicability of the transonic area rule to the case of wings of triangular plan form. To accomplish this objective, measurements were made in a transonic wind tunnel of the zero-lift drag of a family of triangular wings of varying thickness and aspect ratio. To provide a practical means of support in the tunnel the wings were centrally mounted on a long cylindrical body. The body geometry was chosen to simulate an infinite cylinder, and the ratio of body diameter to wing span was held constant to preserve an affine relationship for the wing-body

combinations. These requirements are necessary for the transonic similarity parameters and the method of analysis used in reference 1 to be directly applicable.

SYMBOLS

A	aspect ratio
b	wing span
C_D	zero-lift drag coefficient
ΔC_D	zero-lift drag-rise coefficient
δC_D	correction to C_D due to interference
C_p	pressure coefficient
c	wing chord
D	zero-lift drag
D_w	zero-lift wave drag
ΔD	zero-lift drag rise
d	body diameter
l	body length
M	free-stream Mach number
M.A.C.	mean aerodynamic chord
q	free-stream dynamic pressure
S	plan-form area, including portion within body
S_c	cross-sectional area
S_m	maximum cross-sectional area
$\frac{t}{c}$	maximum thickness ratio of wing
x	body longitudinal coordinate, measured from body nos
α	angle of attack, deg

APPARATUS

The experimental study was made in the Ames 2- by 2-foot transonic wind tunnel, which is of the closed-circuit, variable-pressure type. The wind tunnel is fitted with a flexible nozzle followed by a ventilated test section of 6-percent open area which permits continuous choke-free operation from 0 to 1.4 Mach number. Condensation effects are rendered negligible by maintaining the air in the tunnel at a specific humidity of less than 0.0003 pound of water per pound of air.

Six wing-body models having triangular wings of aspect ratios, thickness ratios, and other characteristics as given in figure 1 were constructed of steel. NACA 63A00X airfoil sections were employed in the streamwise direction. Included in figure 1 is a sketch of the body of revolution which consisted of a Karman ogive nose of fineness ratio 6 and a cylindrical afterbody. The models were mounted in the wind tunnel on a sting as shown in figure 2(a). The models spanned 42 percent of the test-section height and blocked from 0.34 to 0.64 percent of the test section cross-sectional area.

In order to evaluate the drag rise of the wings to a relatively high degree of accuracy, the wings were supported by an electrical strain-gage balance independently of the body. Figure 2(b) is a photograph of the model parts, while figure 3 shows a cross section through the body. The body was constructed in the form of a sleeve, fitting over the strain-gage balance, and attached directly to the wind-tunnel sting. The wings were attached to flush-surfaced ribs extending through slots in the sides of the body; the ribs were in turn rigidly attached to the forepart of the balance. Clearance between the body and the ribs was less than 0.005 inch. An electrical fouling circuit was provided for detecting any contact between the body and the parts of the model which were attached to the balance.

TESTS

The test program consisted of the measurement of the zero-lift drag of the six wings when mounted on the body, the measurement of the friction drag of the flush surfaces of the ribs to which the wings were attached, and a special test consisting of the measurement of the pressure distribution along the cylindrical portion of the body with no wings installed. The latter test was performed to determine the magnitude and extent of pressure perturbations in the flow field in the region occupied by the wings and is discussed in detail in the Appendix.

The procedure followed in running the tests was to set the angle of attack of the model at 0° and operate the wind tunnel through the desired range of Mach numbers. Drag data were obtained at 22 Mach numbers ranging

from 0.6 to 1.4. A Reynolds number of 1.0 million, based on the mean aerodynamic chord of the exposed wing plan form of each model, was held constant for the tests.

Test data were taken with and without boundary-layer tripping devices on the wings and body. Since there was no essential difference in the drag rise of the wings under these two conditions, only the results from the tests without tripping devices are presented.

REDUCTION AND PRECISION OF DATA

All drag coefficients are based on the wing area including the portion within the body.

The total drag reported herein is the drag of the wings as measured less a portion of the friction drag measured when the body was tested alone, that is, without wings attached to the flush surfaces. The portion of the friction drag subtracted was determined by computing the ratio of the exposed area of the flush surfaces with wings attached to the total flush-surface area. This correction was small percentagewise and in no case exceeded a drag-coefficient value of 0.0012.

To obtain the sonic drag rise, the subsonic drag at $M = 0.6$ was subtracted from the sonic drag value. Since the transonic similarity parameters, used herein to present the data at sonic speed, apply to the pressure or wave drag, the tacit assumption is that the drag rise approximates the pressure drag. The reasoning involved, of course, is that the change in friction drag over the Mach number range of interest was negligible and that no serious amount of flow separation occurred.

Further small corrections were made to the drag data due to the presence of pressure perturbations in the flow in the region of the wings caused by body-nose and wind-tunnel-wall interference. In order to indicate the order of magnitude of corrections of this type, the total drag data presented subsequently are shown with and without these interference corrections applied.

Apart from the small systematic corrections to the data discussed above, certain random errors of measurement exist which determine the precision or repeatability of the data. An analysis of the precision of the Mach number, angle of attack, and drag coefficient has been made, and the random uncertainties at three representative Mach numbers are given below:

	M = 0.8	M = 1.0	M = 1.2
M	±0.003	±0.004	±0.002
α	±.02 ^o	±.02 ^o	±.02 ^o
C _D	±.0002	±.0003	±.0002

RESULTS AND DISCUSSION

The experimental results for the six triangular plan form wings in terms of total drag coefficient versus Mach number are presented in figure 4. Included in the figure is the effect on the drag coefficient of the interference pressure field discussed previously. It is to be noted that the interference effect, while small for most of the wings, is most pronounced in the low supersonic speed range where transonic wind-tunnel interference has previously been known to exist. Since obtaining accurate data at sonic speed was the primary concern of the present tests, it is of particular interest to note that the interference effect at a Mach number of 1 is negligible.

To define the range of applicability of the transonic area rule to affinely related wings, the geometric parameter used at $M = 1.0$ is $A(t/c)^{1/3}$. The limitation to the area rule can be found by plotting the variation of the reduced drag-rise coefficient, $\Delta C_D / (t/c)^{5/3}$, with $A(t/c)^{1/3}$, the limiting value being given by the point where the curve formed by the data points departs from a straight line through the origin. A detailed explanation of the reasoning behind the foregoing statement is given by Spreiter in reference 1. A short summary of the explanation is as follows:

The transonic area rule states that the variations of $\Delta D/q$ with Mach number are the same for all low-aspect-ratio wing-body combinations having the same longitudinal area distribution $S_c(x)$. In notational form and from a slightly different point of view,

$$\frac{\Delta D}{qc^2} = f \left[M, \frac{S_c(x/c)}{c^2} \right] \quad (1)$$

If attention is confined at $M = 1.0$ to a family of affinely related wings so that the area distribution is specified by giving, for instance, the chord, c and the ratio S_m/c^2 or its equivalent in terms of aspect ratio and thickness ratio, equation (1) can be rewritten as

$$\frac{\Delta D}{qc^2} = \left(\frac{S_m}{c^2} \right)^2 f \left[A \left(\frac{t}{c} \right) \right] \quad (2)$$

where S_m is the maximum cross-sectional area. This statement says that the drag rise at a Mach number of 1 for a family of affinely related wings is proportional to the product of the square of the maximum cross-sectional area times some function of the product of the aspect ratio and thickness ratio.

In contradistinction, the transonic similarity rule states that the pressure drag at $M = 1.0$ of an affinely related family of wings with symmetric sections is given by

$$\frac{D_w}{qc^2} = \left(\frac{S_m}{c^2}\right)^2 f\left[A\left(\frac{t}{c}\right)^{1/3}\right] \quad (3)$$

The assumption is made that the drag rise closely approximates the wave drag at $M = 1.0$, and correspondingly, $\Delta D/qc^2$ may be considered equal to D_w/qc^2 . The argument then proceeds that if both rules, equations (2) and (3), are to be true, the drag depends on neither $f[A(t/c)]$ nor $f[A(t/c)^{1/3}]$. This leads to the relation

$$\frac{\Delta D}{qc^2} = \left(\frac{S_m}{c^2}\right)^2 K \quad (4)$$

where K is some constant. Equation (4) can be rewritten as

$$\frac{\Delta C_D}{(t/c)^{5/3}} = KA\left(\frac{t}{c}\right)^{1/3} \quad (5)$$

which, of course, defines a straight line through the origin on a figure where the terms on the right and left of equation (5) are the abscissa and ordinate, respectively.

Shown in figure 5 is the variation of the reduced sonic drag-rise coefficient, $\Delta C_D/(t/c)^{5/3}$ versus $A(t/c)^{1/3}$ for the present family of triangular wings. For comparative purposes, the previous data (ref. 1 or 2) for wings with rectangular plan form are included. The figure shows that for triangular wings, the data are in agreement with the transonic area rule for values of $A(t/c)^{1/3}$ up to 1.3. This limit is not too well defined, however, since the divergence of the data from a straight line at higher values of $A(t/c)^{1/3}$ proceeds slowly, and is not as pronounced as it is for rectangular wings where disagreement occurs abruptly at $A(t/c)^{1/3} = 1.0$.

As a further aid in visualizing the form of the drag curves in figure 5, it should be mentioned in passing that as $A(t/c)^{1/3} \rightarrow \infty$, the reduced drag-rise coefficient for both plan forms asymptotically approaches the same two-dimensional value.

The foregoing discussion has served to show, as was also discussed in reference 1, that the usefulness of the transonic area rule can be extended beyond the original statement of the rule. The drag rise at sonic speed of a member of an affinely related family of wings can be predicted from knowledge of the sonic drag rise of another member of the family, if both wings are within the range of applicability of the transonic area rule. This result, which uses both the transonic similarity rule and the transonic area rule, cannot be deduced from either rule alone.

It might at first be inferred that a direct drag correspondence at $M = 1.0$ would exist between the present triangular wings with $A(t/c)^{1/3} < 1.3$ and their equivalent bodies, which in the present case are recognized as being represented by an infinite cylindrical body with an axially symmetric bump having the same longitudinal area distribution as the wing. Actually, however, as has been investigated theoretically in reference 3, this correspondence does not always hold. In fact, for the present triangular wings, calculations based upon equation (153) of reference 3 indicate that the sonic drag rise of the equivalent body is approximately half that of the wing. This difference is associated with discontinuities in the longitudinal area distribution that occur at the trailing edge of the wing, and can be removed (at least theoretically) by reducing the trailing-edge angle of the wing sections to zero by cusping the trailing-edge region.

It might also be inferred from the present results that for the triangular wings tested with $A(t/c)^{1/3} < 1.3$, mounted on an area-rule-compensated, infinite cylindrical body, the sonic drag rise would be zero. Unfortunately, the difficulty that arises between the wing and its equivalent body discussed in the previous paragraph would occur and the zero drag-rise condition would not be obtained. However, the difficulty can again be removed in the manner mentioned above.

CONCLUDING REMARKS

The results of an experimental investigation performed to determine the range of applicability of the transonic area rule for wings with triangular plan form, NACA 63A00X airfoil sections in the streamwise direction, and centrally mounted on a simulated infinite cylindrical body, show that the data at sonic speed are in agreement with the transonic area rule for values of aspect ratio times thickness ratio to the one-third power [$A(t/c)^{1/3}$] up to 1.3. This result applies strictly for the conditions stated above. However, it is to be expected that changes in wing section, or body diameter to wing span ratio (even for a body diameter to wing span ratio of zero), would not alter the result significantly.

It might be inferred that the limitation found, $A(t/c)^{1/3} = 1.3$, defines the range over which the present triangular wings and the corresponding equivalent bodies would have the same sonic drag rise, and also the range for which an area-rule-compensated wing-body combination consisting of an infinite cylindrical body and a triangular wing would have zero drag rise at sonic speed. It is pointed out, however, that the calculated flow in the region of the trailing edge contains discontinuities, and for these drag relations to be satisfied, cusping of the trailing-edge region would be necessary.

Ames Aeronautical Laboratory
National Advisory Committee for Aeronautics
Moffett Field, Calif., Sept. 25, 1956

APPENDIX

EVALUATION OF BODY-NOSE AND WIND-TUNNEL-WALL INTERFERENCE

Experimental measurements were made of the pressure distribution along the cylindrical portion of the body surface in the region normally occupied by the wings. The purpose of the test was to determine approximately the effect of the expected interference pressure field on the drag coefficient of the wings. Since the desired test shape is represented by an infinite cylindrical wing-body combination with a uniform flow field approaching the wings, any deviation from these conditions due to the presence of the body nose or due to interference from the tunnel walls caused by the presence of the body, or, for that matter, by the wings themselves, would be expected to cause errors in the measured drag. As there is no direct way of evaluating the interference effect from the wings, only the effect of the body has been evaluated.

The test consisted of measuring the surface pressure at 14 locations along the body. Angle of attack and angle of yaw were adjusted to zero. The Mach number was varied over the same range and adjusted to the same values as for the tests performed with the wings. Data were obtained at two values of Reynolds number, one corresponding to the same Reynolds number per unit length as used for wing A and the other corresponding to the value used for wing F. The results of the tests are presented in figure 6. Only the data obtained for the Reynolds number corresponding to the value used for wing F are shown, since the effect of Reynolds number on the pressure distribution was minor. The figure shows that for subsonic Mach numbers the pressure perturbations along the body were negligible, whereas for supersonic flow, particularly for Mach numbers between 1.02 and 1.12, the pressure perturbations are large and, correspondingly, the effect on the drag of the wings would be expected to be significant.

To compute the effect on the drag coefficient of the wings the following simplifying assumptions were made: (1) the addition of the wings to the configuration will not change the amount of interference present (i.e., the additional flow field due to the wings adds linearly to the existing field), and (2), the pressure distribution measured on the body is assumed to extend radially at least out to the tips of the wings with no change in characteristics. These assumptions represent a fair approximation to the true state of affairs at transonic Mach numbers, but become increasingly in error as the Mach number is raised to higher supersonic values. The drag corrections to be computed, therefore, can only be considered approximate and, particularly at the higher Mach numbers, represent only the order of magnitude of the actual corrections.

The drag corrections were computed by multiplying the experimental pressure distribution, $C_p(x)$, by the derivative of the longitudinal area distribution, $S_c'(x)$, of the wings and then integrating the result. In notational form,

$$\delta C_D = \frac{1}{S} \int_0^c C_p(x) S_c'(x) dx$$

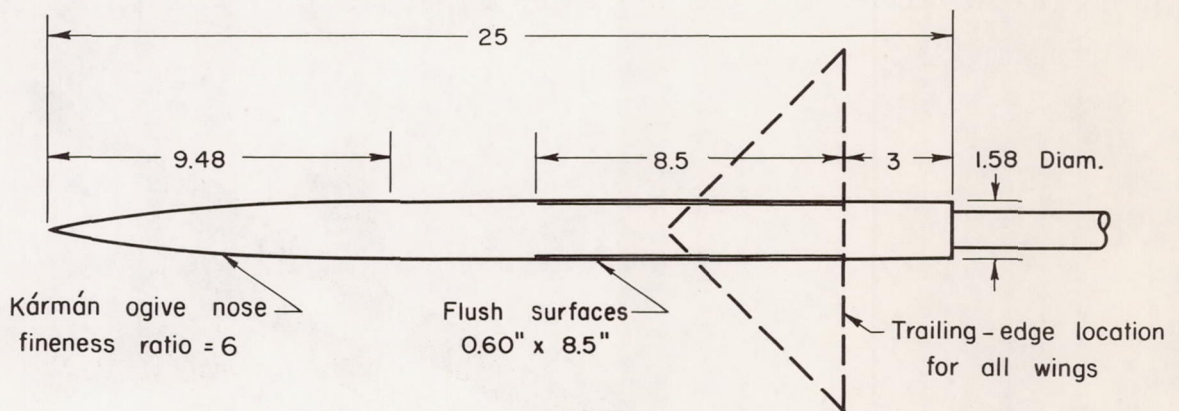
where S is the reference plan-form area. The results of the computations are illustrated by the difference between the two sets of curves shown in figure 4. It is to be noted that the maximum corrections occur in the low supersonic Mach number range where wind-tunnel interference has previously been known to exist. The corrections are smaller at the higher Mach numbers where the accuracy of the corrections is poor.

REFERENCES

1. Spreiter, John R.: On the Range of Applicability of the Transonic Area Rule. NACA TN 3673, 1956. (Supersedes NACA RM A54F28)
2. McDevitt, John B.: A Correlation by Means of the Transonic Similarity Rules of Experimentally Determined Characteristics of a Series of Symmetrical and Cambered Wings of Rectangular Plan Form. NACA Rep. 1253, 1955. (Supersedes NACA RM's A51L17b and A53G31)
3. Heaslet, Max. A., and Spreiter, John R.: Three-Dimensional Transonic Flow Thoery Applied to Slender Wings and Bodies. NACA TN 3717, 1956.

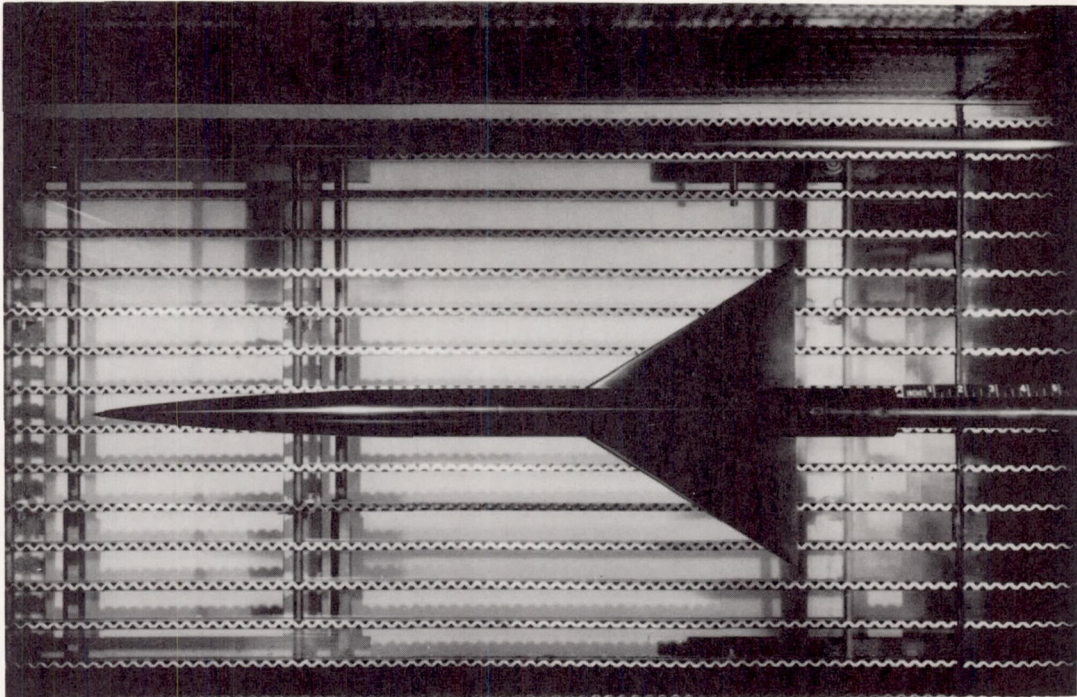
Wing	(t/c)	A	$A (t/c)^{\frac{1}{3}}$	Chord at \bar{C} of body	Span	M.A.C. exposed wing	Total wing area
A	.04	2.046	.7	9.771	10	6.473	48.84
B	.06	2.556	1.0	7.830	10	5.220	39.16
C	.06	3.322	1.3	6.023	10	4.016	30.12
D	.06	4.090	1.6	4.894	10	3.263	24.47
E	.06	4.856	1.9	4.121	10	2.747	20.61
F	.06	5.624	2.2	3.559	10	2.373	17.80

(a) Table of triangular-wing characteristics; dimensions in inches.



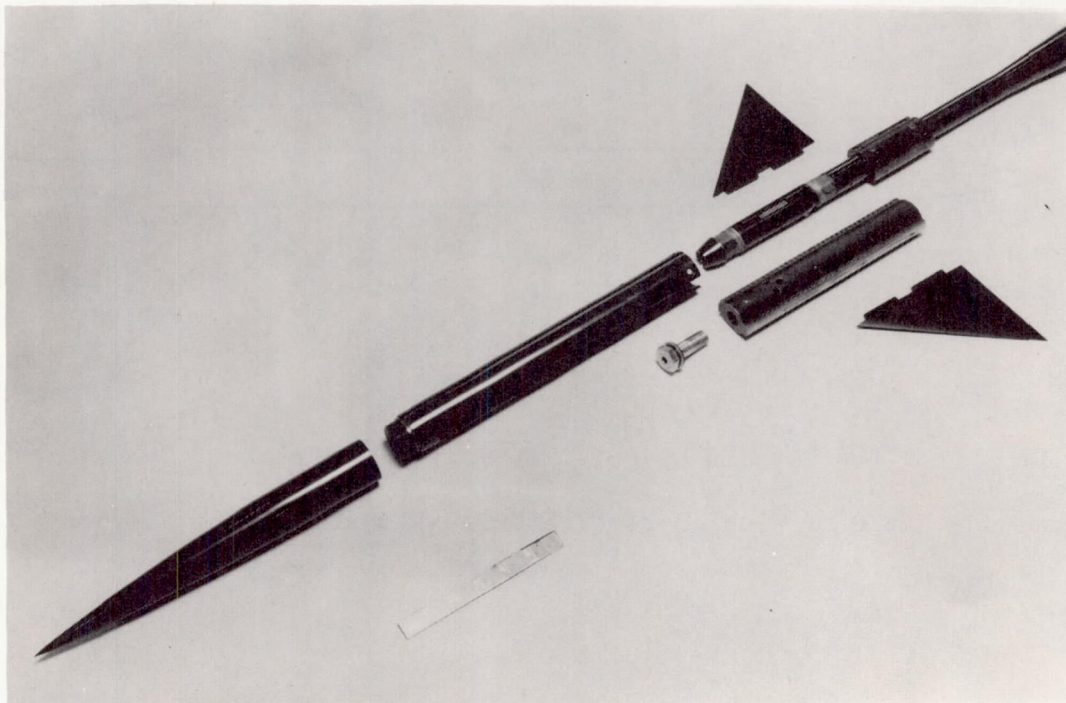
(b) Details of body; dimensions in inches.

Figure 1.- Table of wing characteristics and geometric details of body.



A-20869

(a) Installation in the Ames 2- by 2-foot transonic wind tunnel.



(b) Exploded view of model parts.

A-20906

Figure 2.- Typical model installation and view of model parts.

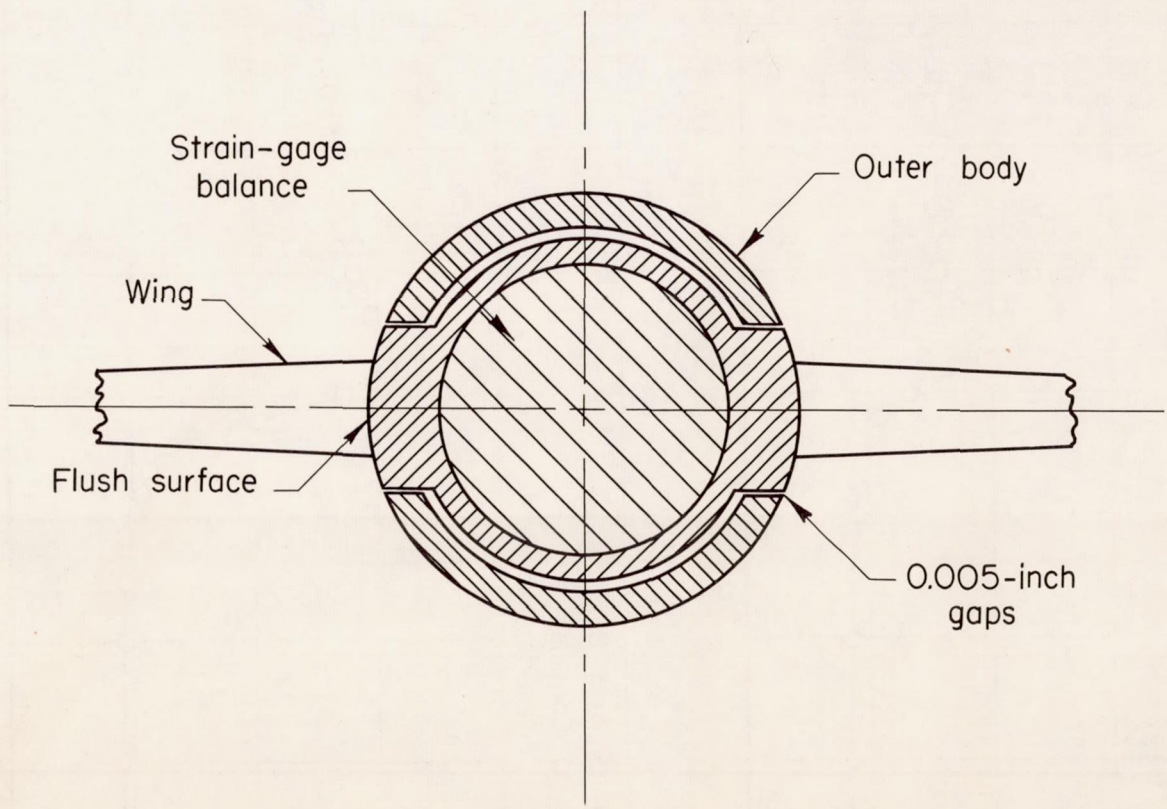


Figure 3.- Cross-sectional view of model construction.

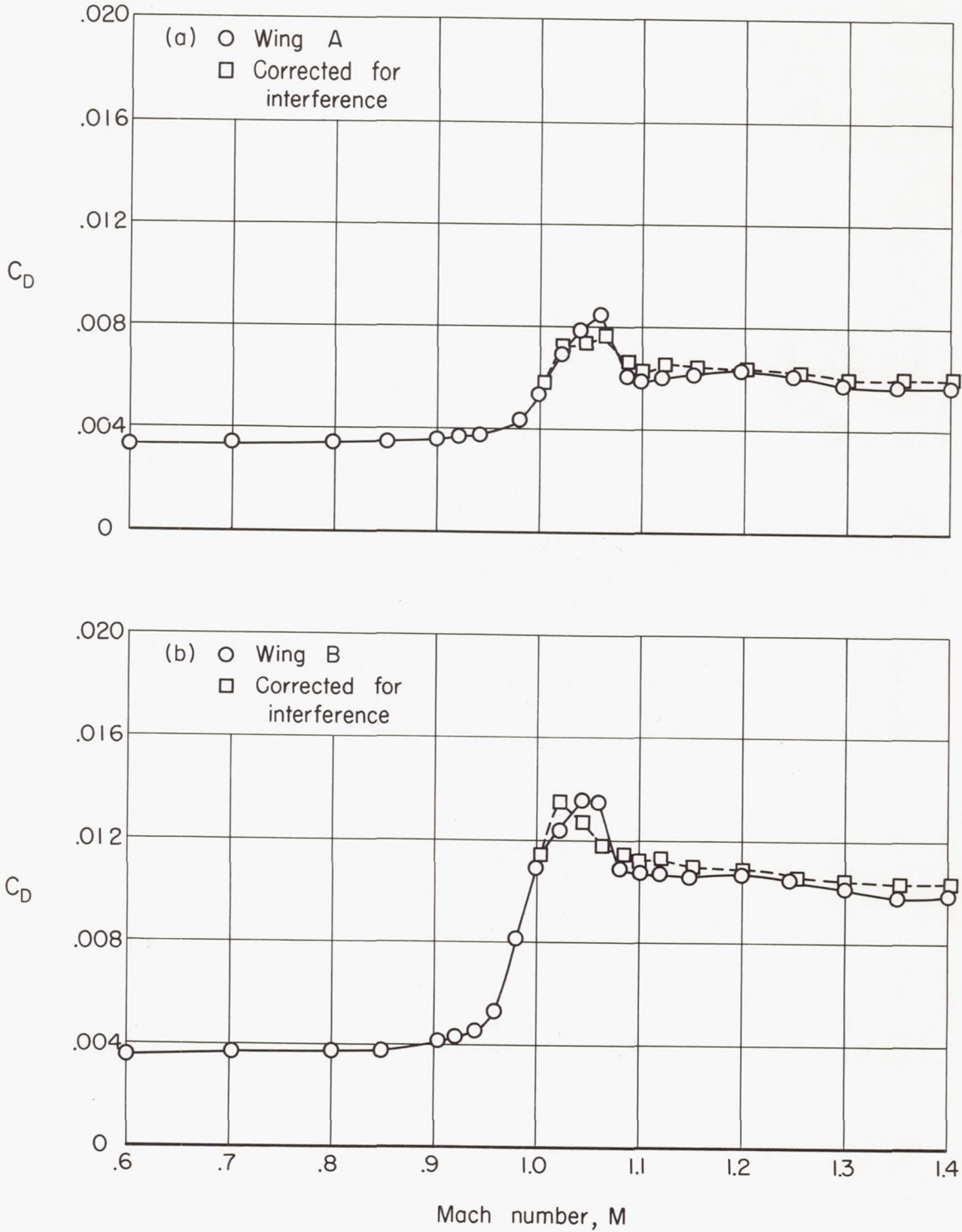


Figure 4.- Variation of zero-lift drag with Mach number for the various wings.

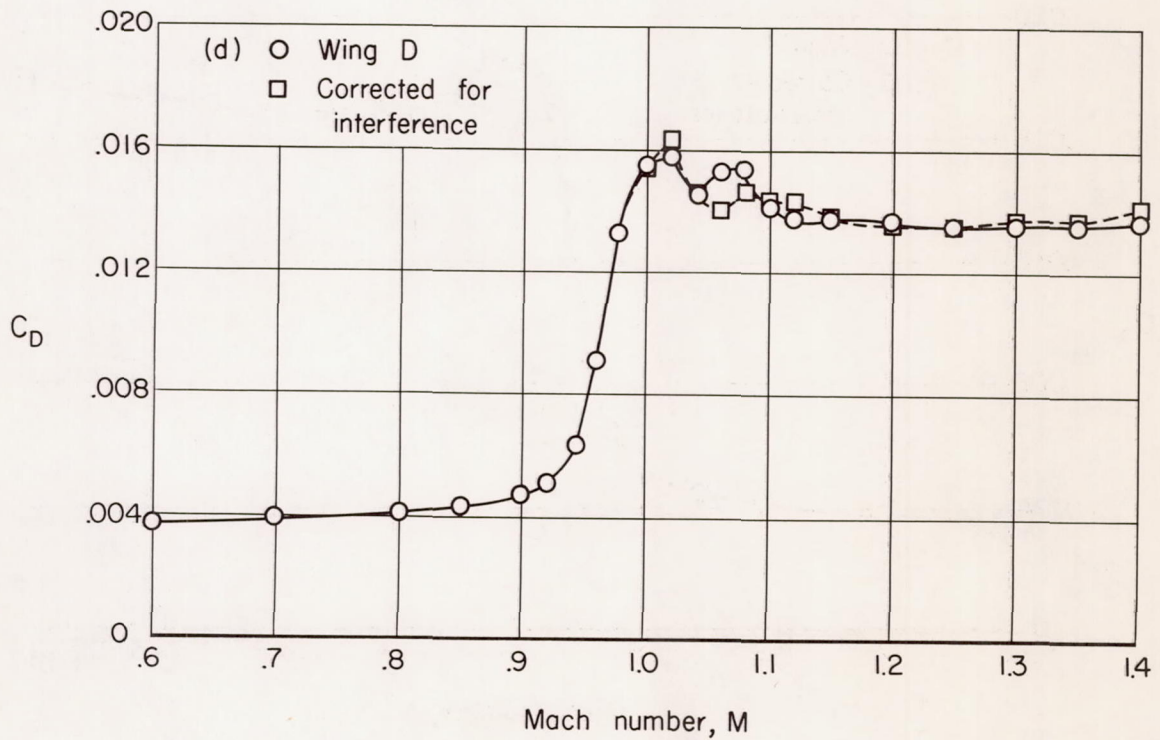
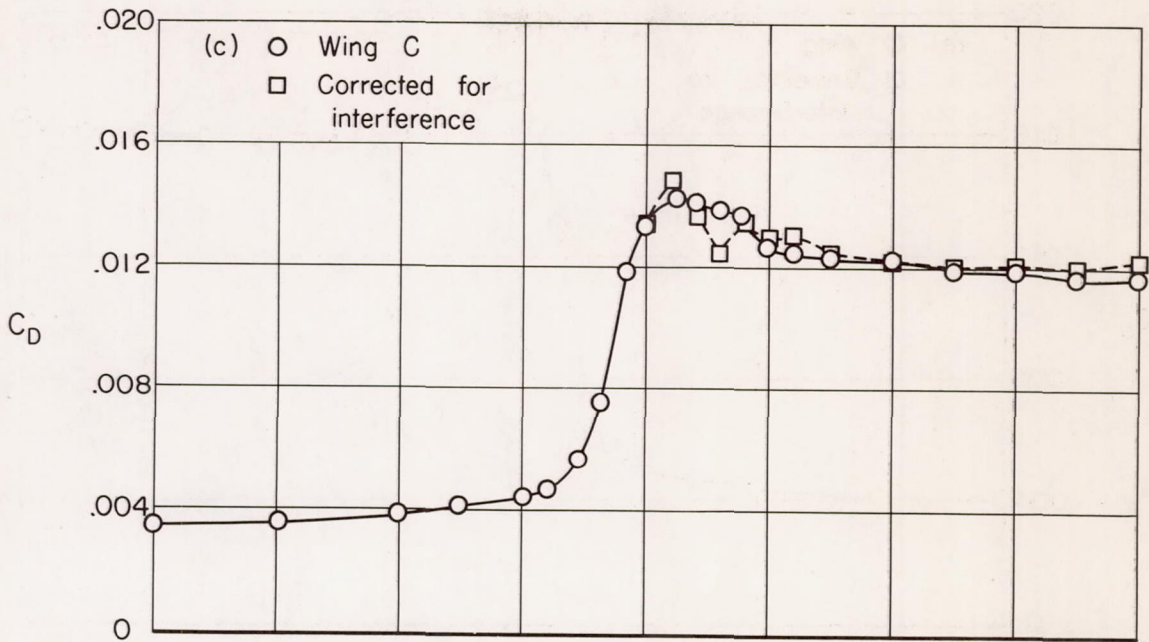


Figure 4.- Continued.

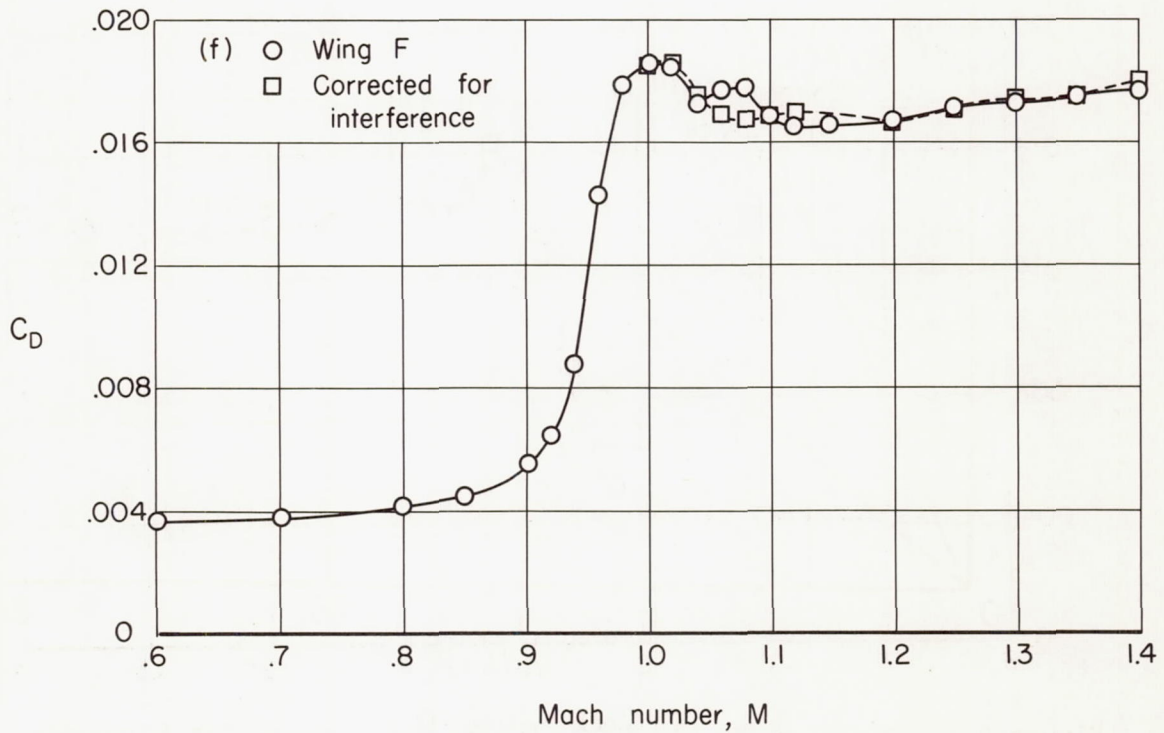
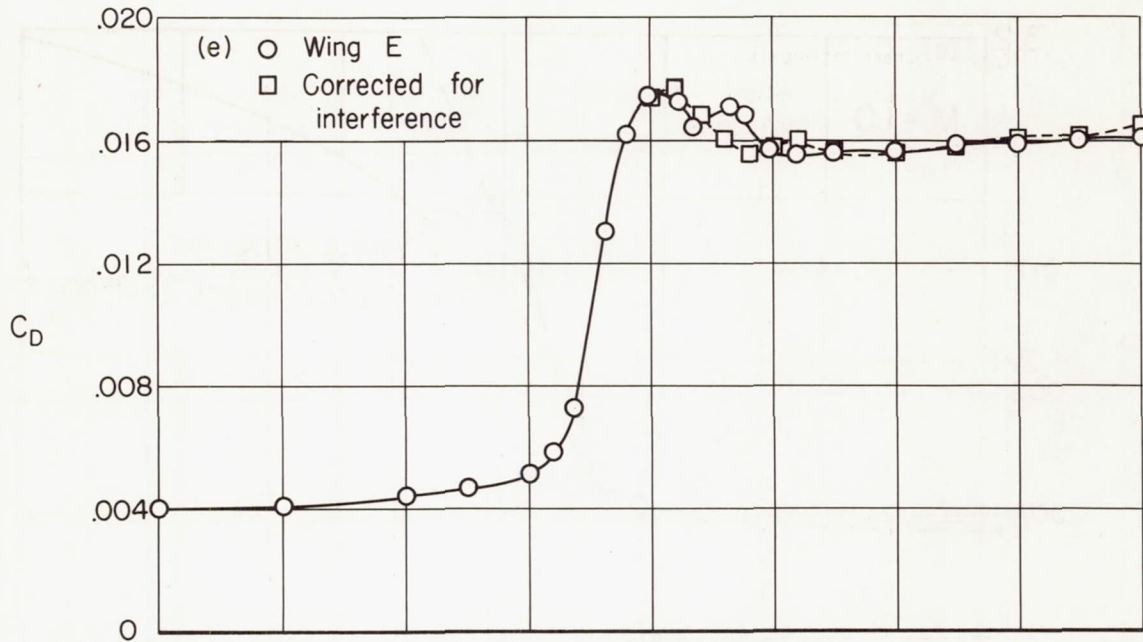


Figure 4.- Concluded.

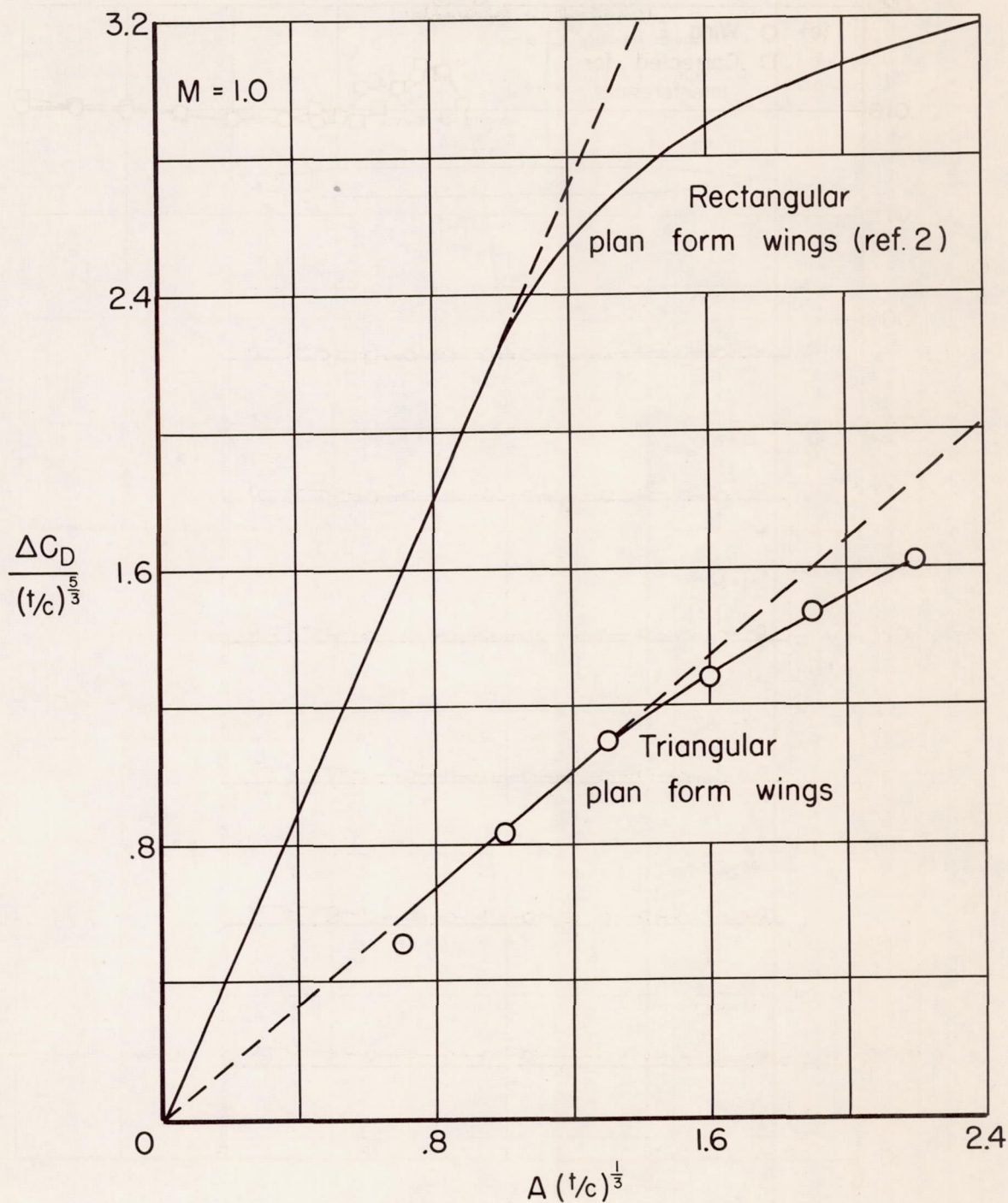
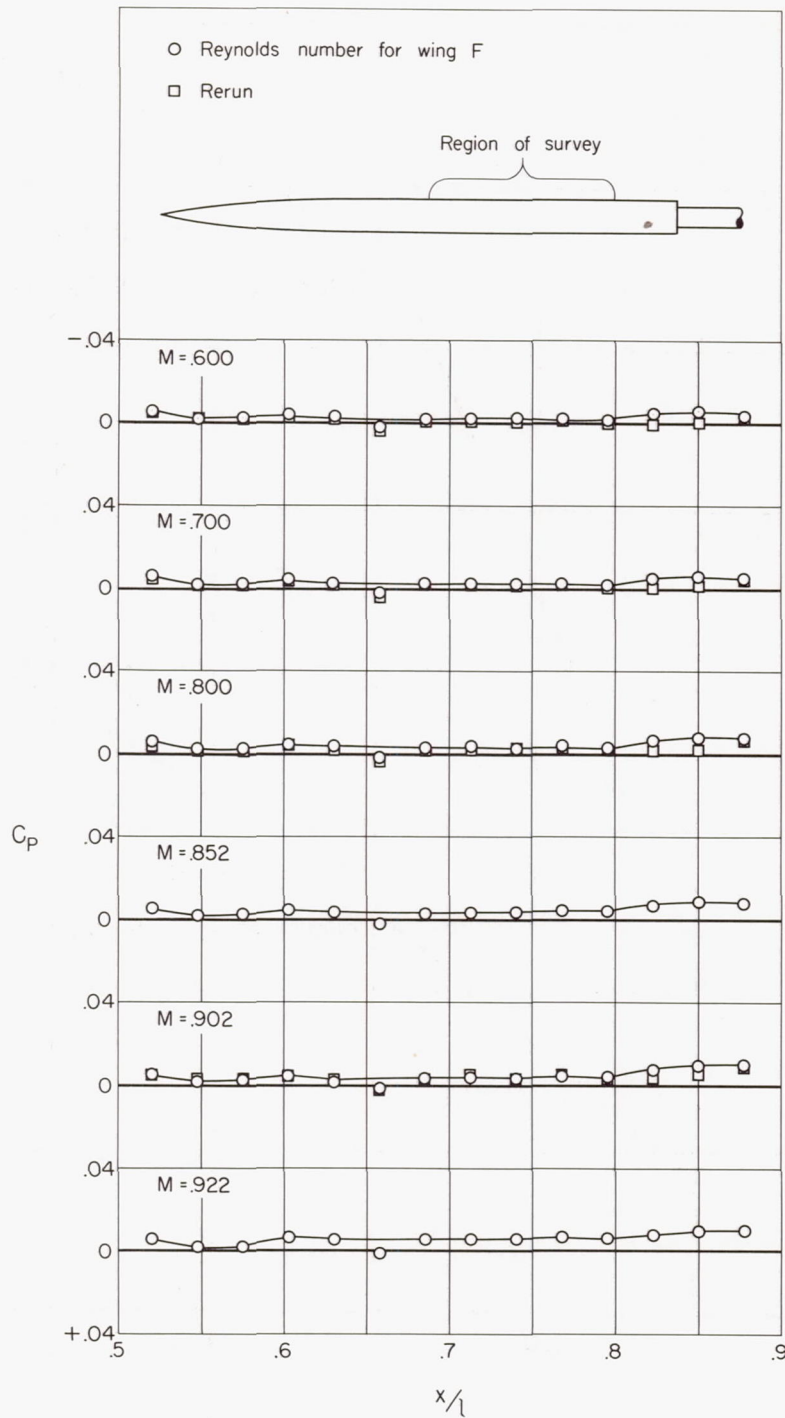
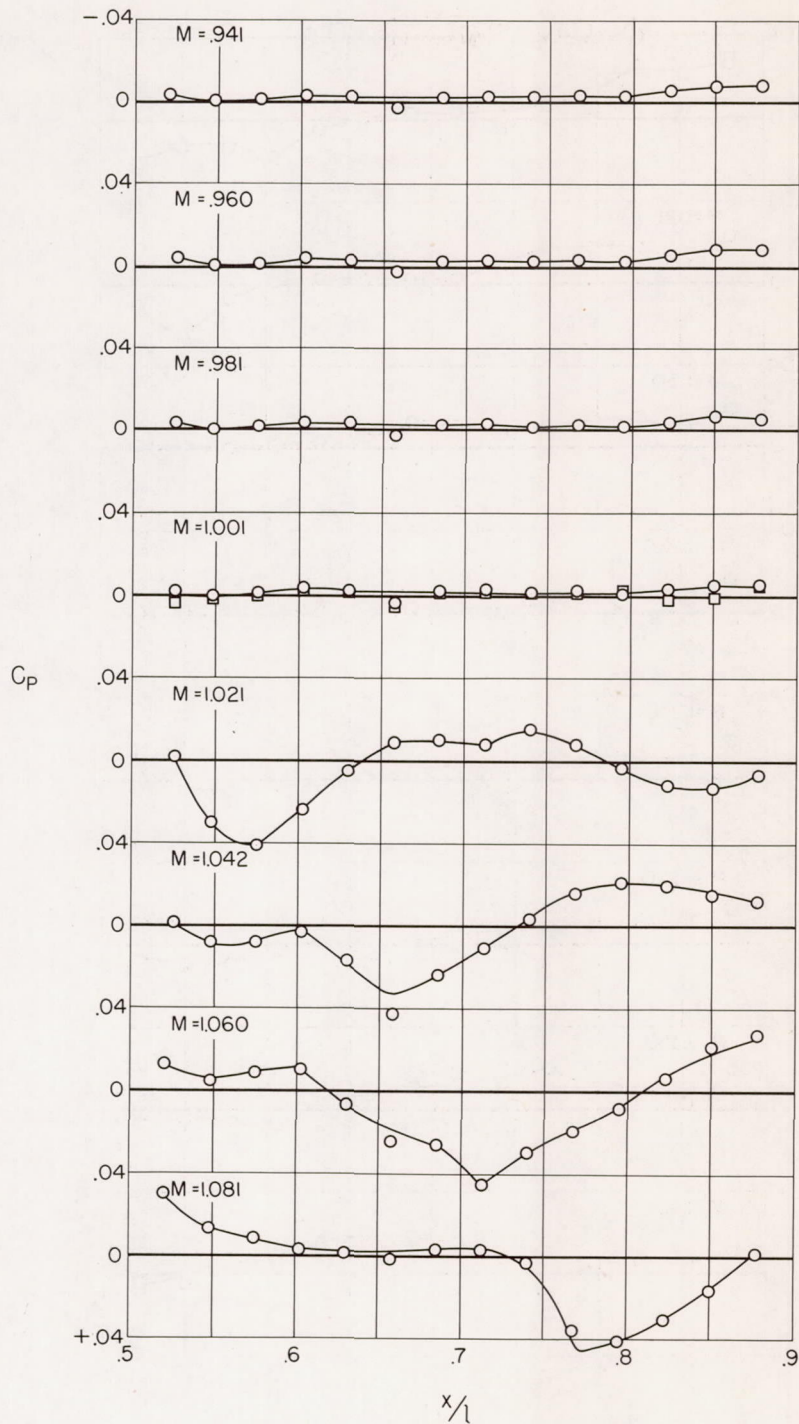


Figure 5.- Comparison of the drag rise at sonic speed for triangular and rectangular plan form wings in transonic similarity form.



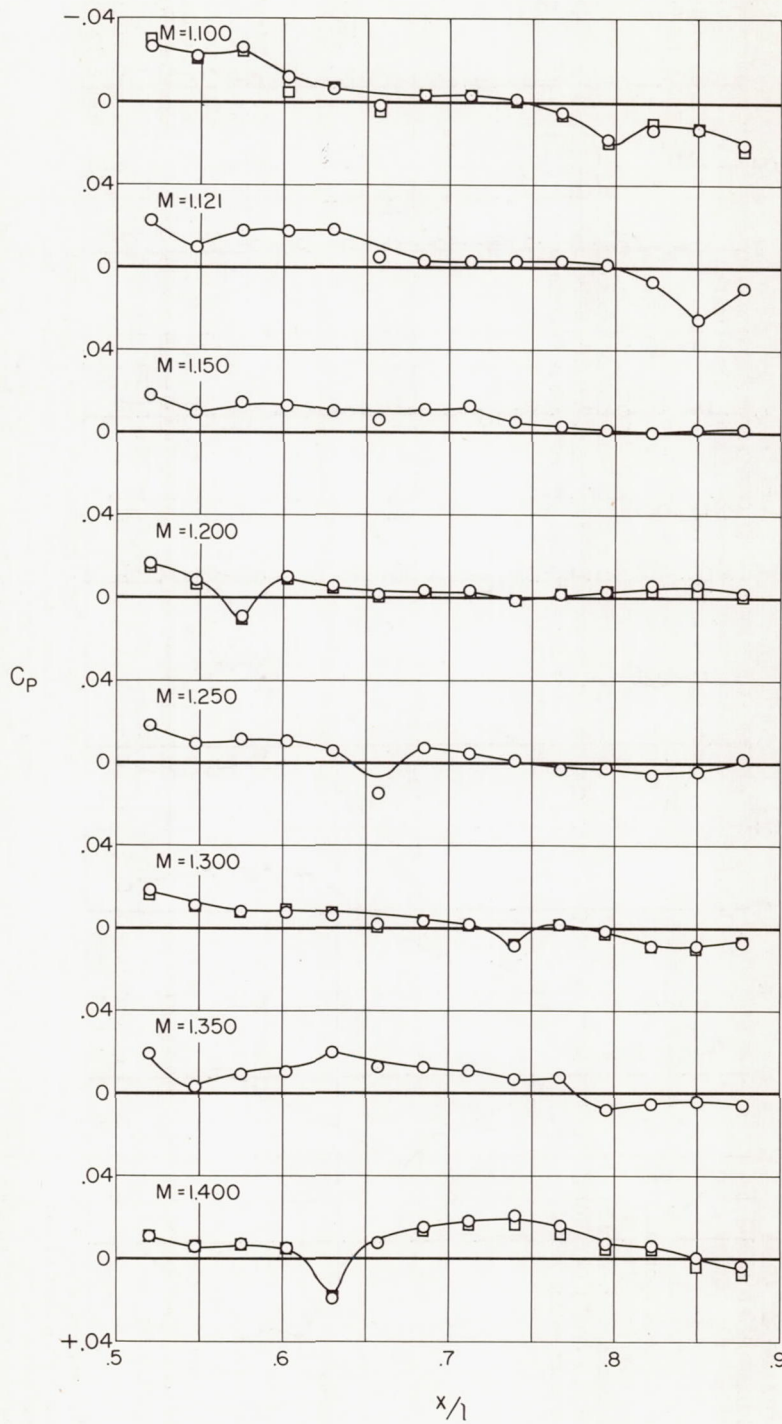
(a) Subsonic Mach numbers.

Figure 6.- Experimental pressure distribution on afterportion of cylindrical body.



(b) Transonic Mach numbers.

Figure 6.- Continued.



(c) Supersonic Mach numbers.

Figure 6.- Concluded.